© 2017. Published by The Company of Biologists Ltd | Development (2017) 144, 2070-2081 doi:10.1242/dev.145755

RESEARCH ARTICLE

Development of the larval lymphatic system in zebrafish

Hyun Min Jung[1], Daniel Castranova[1], Matthew R. Swift[1], Van N. Pham[1], Marina Venero Galanternik[1], Sumio Isogai[2], Matthew G. Butler[1], Timothy S. Mulligan[1] and Brant M. Weinstein[1,*]

ABSTRACT

The lymphatic vascular system is a hierarchically organized complex network essential for tissue fluid homeostasis, immune trafficking and absorption of dietary fats in the human body. Despite its importance, the assembly of the lymphatic network is still not fully understood. The zebrafish is a powerful model organism that enables study of lymphatic vessel development using high-resolution imaging and sophisticated genetic and experimental manipulation. Although several studies have described early lymphatic development in the fish, lymphatic development at later stages has not been completely elucidated. In this study, we generated a new *Tg(mrc1a:egfp)^{y251}* transgenic zebrafish that uses a *mannose receptor, C type 1* (*mrc1a*) promoter to drive strong EGFP expression in lymphatic vessels at all stages of development and in adult zebrafish. We used this line to describe the assembly of the major vessels of the trunk lymphatic vascular network, including the later-developing collateral cardinal, spinal, superficial lateral and superficial intersegmental lymphatics. Our results show that major trunk lymphatic vessels are conserved in the zebrafish, and provide a thorough and complete description of trunk lymphatic vessel assembly.

KEY WORDS: Zebrafish, Mrc1a, Spinal lymphatic, Lateral lymphatic, Collateral cardinal lymphatic, Cardinal lymphatic, Thoracic duct

INTRODUCTION

The lymphatic system is essential for maintaining fluid homeostasis by absorbing water and macromolecules from interstitial spaces within tissues, and dietary lipids and lipid-soluble vitamins from the intestine (Alitalo et al., 2005; Rusznyák et al., 1967; Tammela and Alitalo, 2010). The lymphatic system is also important for immune cell production and trafficking (Baluk et al., 2007; Yoffey and Courtice, 1970). Despite its importance, few published studies have focused on understanding the development and function of lymphatic vessels compared with blood vessels. This is mainly a result of a lack of necessary research tools and difficulties in imaging lymphatic vessels *in vivo*. The lymphatic system also assembles at a relatively late stage compared with the blood vascular system. With the availability of new molecular and experimental tools for studying this 'second vascular system', however, the mechanisms of lymphatic vessel growth and morphogenesis have recently become a subject of intensive investigation in mice and other animal models (Banerji et al., 1999; Fritz-Six et al., 2008; Hermans et al., 2010; Hogan et al., 2009; Hong et al., 2002; Kuchler et al., 2006; Nicenboim et al., 2015; Okuda et al., 2012; van Impel et al., 2014; Wigle and Oliver, 1999; Yaniv et al., 2006). These studies have led to the identification of a number of genes crucial for lymphatic vessel formation and function. However, our understanding of lymphatic vessel development is still incomplete, and studying lymphatic networks in living animals remains a challenging task.

Previous studies have shown that the zebrafish lymphatic system shares many of the morphological, molecular and functional characteristics of lymphatic vessels in other vertebrates (Cha et al., 2012; Flores et al., 2010; Hogan et al., 2009; Kuchler et al., 2006; Mulligan and Weinstein, 2014; Nicenboim et al., 2015; Okuda et al., 2012; Venero Galanternik et al., 2016; Yaniv et al., 2006, 2007). Transgenic reporter lines have provided powerful tools for imaging and studying lymphatic development in the optically clear zebrafish embryo (Jung et al., 2016). Lymphatic vessels were initially observed in zebrafish using the pan-endothelial *Tg(fli1a:egfp)^{y1}* transgenic line (Lawson and Weinstein, 2002; Yaniv et al., 2006). A number of double-transgenic lines have also been used to differentiate between blood and lymphatic vessels, including *Tg(fli1a:egfp)^{y1}, Tg(kdrl:Hsa.HRAS-mCherry)* and *Tg(flt1:yfp), Tg(kdrl:mcherry)* double transgenics (Hogan et al., 2009) and the *Tg(fli1a:egfp)^{y1}, Tg(kdrl:mcherry)* line (Cha et al., 2012). Although none of the transgenes used in these pairs is specific for lymphatic vessels, the transgene combinations used permit distinction between blood and lymphatic vessels. More recently, transgenics have been developed that mark the lymphatic vasculature with at least some specificity, including *Tg(stabilin:YFP)^{hu4453}* (Hogan et al., 2009), *Tg(lyve1:egfp)^{nz15}* (Okuda et al., 2012), *Tg(flt4^{BAC}:mCitrine)^{hu7135}* (van Impel et al., 2014) and *Tg(prox1aBAC:KalTA4-4xUAS-E1b:uncTagRFP)^{nim5}* (van Impel et al., 2014), providing additional useful tools for studying lymphatics in the fish. Previous work from our laboratory and other groups has provided details on the mechanisms of formation of early larval lymphatics in the zebrafish during the first 5 days of development (Astin et al., 2014; Bussmann et al., 2010; Cha et al., 2012; Hogan et al., 2009; Kuchler et al., 2006; Nicenboim et al., 2015; Okuda et al., 2012; van Impel et al., 2014; Yaniv et al., 2006), as well as an initial description of later-stage intestinal lymphatics and some of the later-stage trunk lymphatics (Okuda et al., 2012). However, the formation of later-developing lymphatic structures in the zebrafish remains incompletely described.

Mannose receptor (MR, CD206) is a transmembrane glycoprotein that belongs to the C-type lectin family. In mammals, mannose receptor, C type 1 (Mrc1) is strongly expressed in macrophages and dendritic cells, prominently in lymphatics (Taylor et al., 2005b), and is involved in lymphocyte migration (Irjala et al., 2001; Marttila-Ichihara et al., 2008; Salmi et al., 2013), but is also expressed in sinusoidal endothelial cells (Takahashi et al., 1998), venous sinuses of the human spleen (Martinez-Pomares et al., 2005), and a subset of venous endothelial cells (Linehan et al., 1999). In zebrafish, *mrc1a* is expressed in

[1]Division of Developmental Biology, Eunice Kennedy Shriver National Institute of Child Health and Human Development, National Institutes of Health, Bethesda, MD 20892, USA. [2]Department of Anatomy, School of Medicine, Iwate Medical University, Morioka 020-8505, Japan.

*Author for correspondence (flyingfish2@nih.gov)

B.M.W., 0000-0003-4136-4962

Received 14 October 2016; Accepted 24 April 2017

Development (2017) 144, 2070-2081 doi:10.1242/dev.145755

primitive veins at early stages of zebrafish development (Wong et al., 2009), but its expression has not been investigated at later stages when lymphatic vessels develop.

Here, we report a *Tg(mrc1a:egfp)*^{y251} transgenic zebrafish line that uses the *mrc1a* promoter to drive robust EGFP expression in both developing and established lymphatic vessels. We show that *Tg(mrc1a:egfp)*^{y251} animals express EGFP in previously described early lymphatic structures such as the thoracic duct. We go on to characterize the formation of well-conserved later-developing trunk lymphatic vessels including the collateral cardinal lymphatics (CCLs), the superficial lateral and intersegmental lymphatics, and the deep spinal lymphatic (SL). Our study provides a thorough anatomical and descriptive foundation for future experimental and genetic investigation of trunk lymphatic development in the zebrafish.

RESULTS

Endogenous *mrc1a* is expressed in primitive veins and lymphatics

In 1-day-old zebrafish, in contrast to the arterial marker *dll4* (Fig. 1A, D), *mrc1a* is strongly expressed in the cardinal vein in the trunk (Fig. 1C,F,H) and in major primitive veins in the head (Fig. 1G), with weak expression in the dorsal aorta (DA) (Fig. 1F) that is rapidly extinguished as development proceeds. No nonvascular expression is apparent at this stage. By 4 days postfertilization (dpf), *mrc1a* is also detected in developing lymphatic structures, including the parachordal lines (PL) in the trunk (Fig. 1H) and the facial lymphatics (FL) in the head (Fig. 1I). Expression of the closely related *mrc1b* gene is not detected at 1 dpf and only weak expression in the posterior cardinal vein (PCV) is detected at 4 dpf (data not shown). Because the expression pattern of *mrc1a* resembles that of *lyve1*, the promoter of which drives lymphatic expression in the zebrafish (Fig. 1B,E) (Flores et al., 2010; Okuda et al., 2012), we examined whether *mrc1a* promoter sequences might be similarly useful to drive primitive venous and lymphatic transgene expression.

We generated a Tol2 transgene construct containing 1.9 kb of DNA from the region immediately 5′ to the *mrc1a* transcription start site, as well as 0.3 kb from intron 19 containing conserved intronic DNA sequences between *mrc1a* and *mrc1b*, and cloned it upstream of *egfp* (Fig. 1J). We then injected this Tol2(*mrc1a:egfp*) transgene into one-cell zebrafish embryos. The Tol2(*mrc1a:egfp*) construct

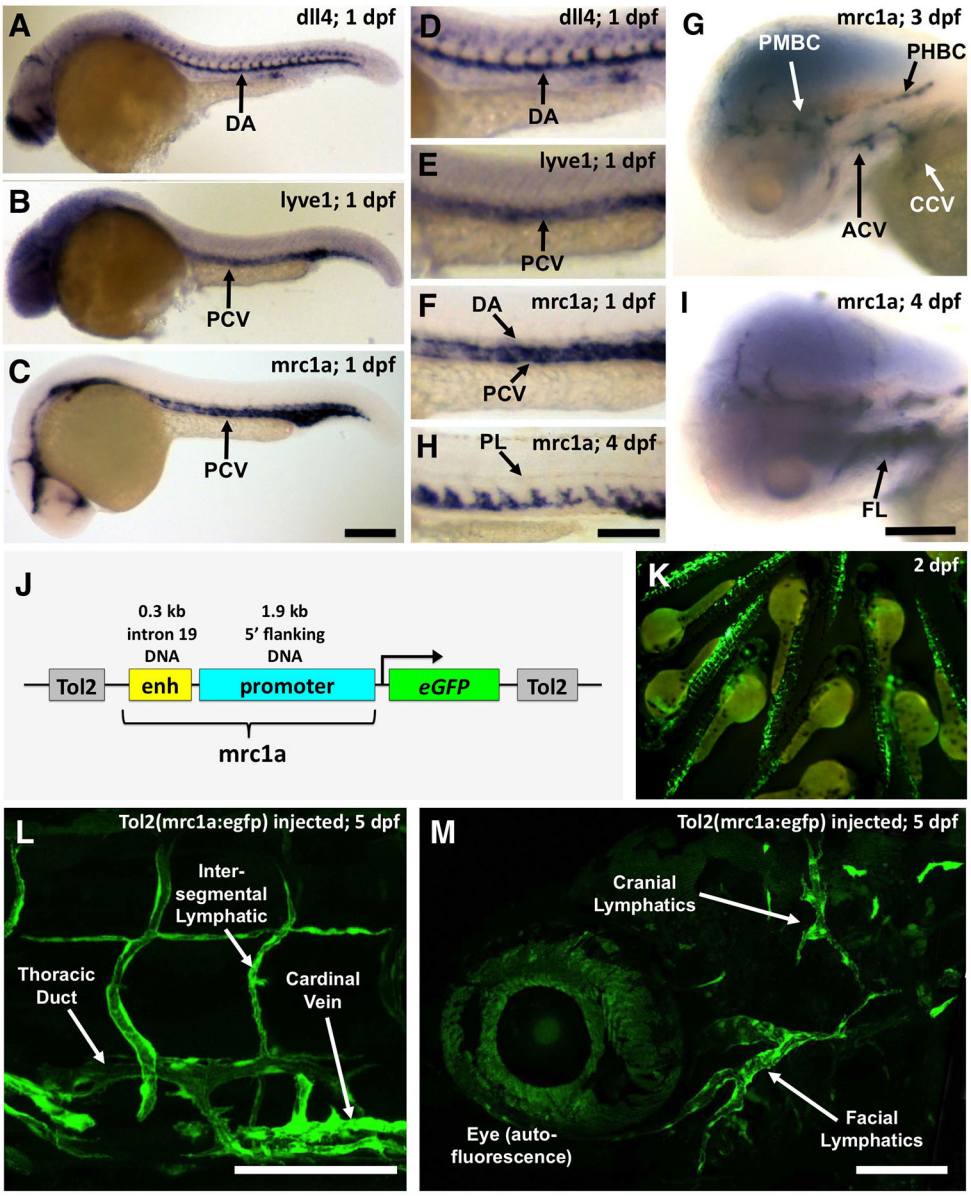

Fig. 1. Zebrafish *mrc1a* is expressed in primitive veins and lymphatics. (A-I) Images of 1-dpf (A-G) and 4-dpf (H,I) wild-type zebrafish subjected to whole-mount ISH, and probed for *dll4* (A,D), *lyve1* (B,E) or *mrc1a* (C,F-I). Images show lateral views of the whole animal (A-C), or higher magnification views of the midtrunk (D-F,H) or head (G,I). (J) Schematic of Tol2(*mrc1a:egfp*) transgene. (K) Epifluorescence micrograph of green vascular fluorescence in Tol2(*mrc1a:egfp*) transgene-injected 2-dpf wild-type animals. (L,M) Confocal micrographs of transgene-positive cells in 5-dpf Tol2(*mrc1a:egfp*)-injected animals, showing labeling of the TD, intersegmental lymphatics, cardinal vein in the trunk (L), and cranial lymphatics and FL in the head (M). ACV, anterior cardinal vein; CCV, common cardinal vein; DA, dorsal aorta; FL, facial lymphatics; PCV, posterior cardinal vein; PHBC, primordial hindbrain channel; PL, parachordal lines; PMBC, primordial midbrain channel. All images are lateral views, rostral to the left. Scale bars: 250 µm (C), 125 µm (H,I,L,M).

Development (2017) 144, 2070-2081 doi:10.1242/dev.145755

drives robust mosaic expression of EGFP in primitive veins and in lymphatic vessels (Fig. 1K-M). We obtained multiple germline founders from Tol2(*mrc1a:egfp*)-injected animals that all exhibited strong, uniform expression of EGFP in primitive veins and lymphatics. The rest of this study describes results obtained using a line generated from one of these founders, *Tg(mrc1a:egfp)^{y251}*. The *mrc1a* promoter sequences we used also drive expression in the maternal germline, since maternal expression of *mrc1a:egfp* in the early embryo was noted in multiple different germline transgenic founders (Fig. S1). Although we found no nonvascular zygotic expression of *mrc1a* (Fig. 1C), and residual maternally contributed EGFP is largely gone by 2 dpf (data not shown), to avoid this maternal expression all of the experiments in the rest of this study were performed using male *Tg(mrc1a:egfp)^{y251}* carriers crossed to wild-type females, resulting in animals with no maternally derived EGFP but robust vascular EGFP expression (Fig. S1).

Tg(mrc1a:egfp)^{y251} transgenic zebrafish express EGFP in veins and lymphatics

We crossed our *Tg(mrc1a:egfp)^{y251}* transgenic line to *Tg(kdrl:mcherry)^{y171}* zebrafish (in which blood vessels are marked with red fluorescence) to generate a *Tg(mrc1a:egfp)^{y251}, Tg(kdrl:mcherry)^{y171}* double-transgenic line, and performed imaging to examine transgene expression in these animals (Figs 2 and 3). Strong primitive venous and lymphatic vascular expression of *mrc1a:egfp* is noted throughout early development (Fig. 2). At 1 dpf, there is strong *mrc1a:egfp* expression in the PCV, as well as some weaker expression in the DA and intersegmental vessels (ISVs) (Fig. 2 and Fig. 3B-D). DA and arterial ISV expression of *mrc1a:egfp* fades away over the next several days, and is mostly undetectable by 3 dpf, but PCV and venous ISV expression of *mrc1a:egfp* remains strong. As described previously (Okuda et al., 2012), facial lymphatic sprouts expressing *mrc1* originate from the common cardinal vein, growing alongside the primary head sinus at 38-55 hours postfertilization (hpf) (Movie 1). By 3 dpf, *mrc1a:egfp* is strongly expressed in developing FL in the head (Fig. 3E-G), and in the newly formed PL in the trunk (Fig. 3H-J), which are vascular cords on both sides of the fish from which other lymphatic vessels

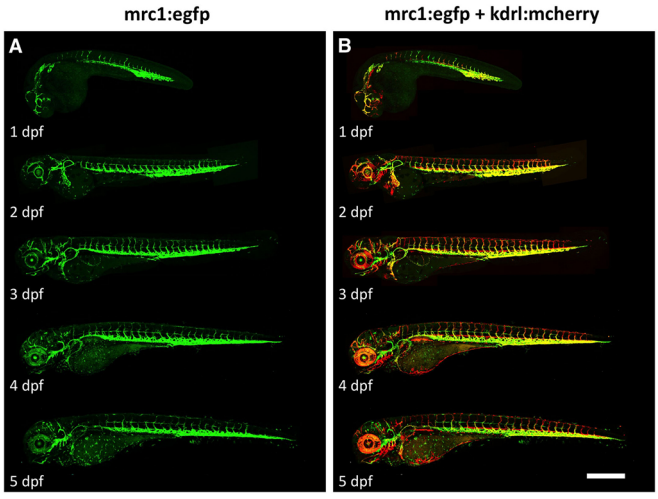

Fig. 2. *Tg(mrc1a:egfp)^{y251}* transgenic zebrafish express EGFP in veins and lymphatics. Confocal images of *mrc1:egfp* green fluorescence (A) and both *mrc1:egfp* green and *kdrl:mcherry* red fluorescence (B) in the same *Tg(mrc1a:egfp)^{y251}, Tg(kdrl:mcherry)^{y171}* double-transgenic animals at 1-5 dpf. All images are lateral views of the entire animal, rostral to the left. Scale bar: 500 µm.

emerge. At 5 dpf, *mrc1a:egfp* expression is observed in the thoracic duct (Fig. 3K-M), a major trunk lymphatic vessel that forms immediately adjacent to the DA in all vertebrates (Kampmeier, 1969; Yaniv et al., 2006). Although the name 'cardinal lymphatic' has been used to describe this vessel in lower vertebrates, we will refer to this vessel as the thoracic duct (TD) hereafter to emphasize its homology to the TD of mammals and in accordance with previous descriptions of this vessel in zebrafish. Although there is overlapping *mrc1a:egfp* and *kdrl:mcherry* expression in large primitive venous blood vessels such as the PCV (Fig. 3B-D), the nonvenous expression patterns of these two transgenes are largely distinct, with that of *Tg(mrc1a:egfp)^{y251}* mostly restricted to lymphatic vessels.

The expression that we observe in the *Tg(mrc1a:egfp)^{y251}* transgenic line resembles that previously reported for the *Tg(lyve1:dsRed)^{nz101}* zebrafish transgenic line (Okuda et al., 2012). We crossed these two lines together to generate a *Tg(mrc1a:egfp)^{y251}, Tg(lyve1:dsRed)^{nz101}* double-transgenic line and performed imaging to directly compare their expression patterns (Fig. 4). We found that the two transgenic lines have extremely similar expression patterns, with comparable labeling of the FL (Fig. 4B-D), PL (Fig. 4E-G) and TD (Fig. 4H-J). We did note a few differences in the expression patterns of the two lines. Strong EGFP fluorescence is evident in the cardinal vein and other primitive veins by ∼24 hpf in the *Tg(mrc1a:egfp)^{y251}* line, whereas robust dsRed fluorescence is not observed until ∼48 hpf in *Tg(lyve1:dsRed)^{nz101}* transgenic animals. EGFP is also expressed in macrophages in the *Tg(mrc1a:egfp)^{y251}* line, most obviously around the head, gut and yolk sac; however, these macrophages are clearly distinguishable from lymphatic vessels (Movie 2). Macrophage expression is not detected in *Tg(lyve1:dsRed)^{nz101}* transgenic fish. In 5-dpf *Tg(lyve1:dsRed)^{nz101}* transgenic animals, but not *Tg(mrc1a:egfp)^{y251}* transgenics, dsRed expression is also noted in the fins, particularly the ventral fins. Apart from these differences, the expression patterns observed in *Tg(mrc1a:egfp)^{y251}* and *Tg(lyve1:dsRed)^{nz101}* transgenic animals are very similar, although the *mrc1a:egfp* line has a substantially stronger fluorescence signal.

We were able to verify that the EGFP-positive vessels we observed in *Tg(mrc1a:egfp)^{y251}* transgenic animals were indeed functional lymphatics using intramuscular injection of Qdot705 quantum dots (Fig. S2 and Movie 3). Qdot705 injected into the head of a 2-month-old *Tg(mrc1a:egfp)^{y251}* zebrafish was rapidly taken up into adjacent *mrc1a:egfp*-positive vessels (Fig. S2A-C). Similarly, Qdot705 injected into the caudal musculature of a 12- to 13-dpf *Tg(mrc1a:egfp)^{y251}* zebrafish could be observed filling the *mrc1a:egfp*-positive TD much further anterior in the midtrunk (Fig. S2D-F and Movie 3). The quantum dots accelerate as they move rostrally through the TD (Fig. S3), eventually draining into the circulation (Movie 4). Together, these data show that the *Tg(mrc1a:egfp)^{y251}* transgenic line provides a robust and reliable transgenic background for assessing the development of the lymphatic vascular system in the zebrafish.

Classical anatomical studies have provided detailed descriptions of major trunk lymphatic vessels conserved throughout vertebrates (Kampmeier, 1969) (Fig. S4). Below, we provide detailed information on the formation and assembly of each of these important lymphatic structures in the developing larval zebrafish.

Formation of the CCLs

Beginning at ∼5-6 dpf, a new pair of *mrc1a:egfp*-positive vascular channels appears in the ventral trunk adjacent and slightly ventral-lateral to the PCV, on either side of the pronephric duct (Fig. 5). In

Development (2017) 144, 2070-2081 doi:10.1242/dev.145755

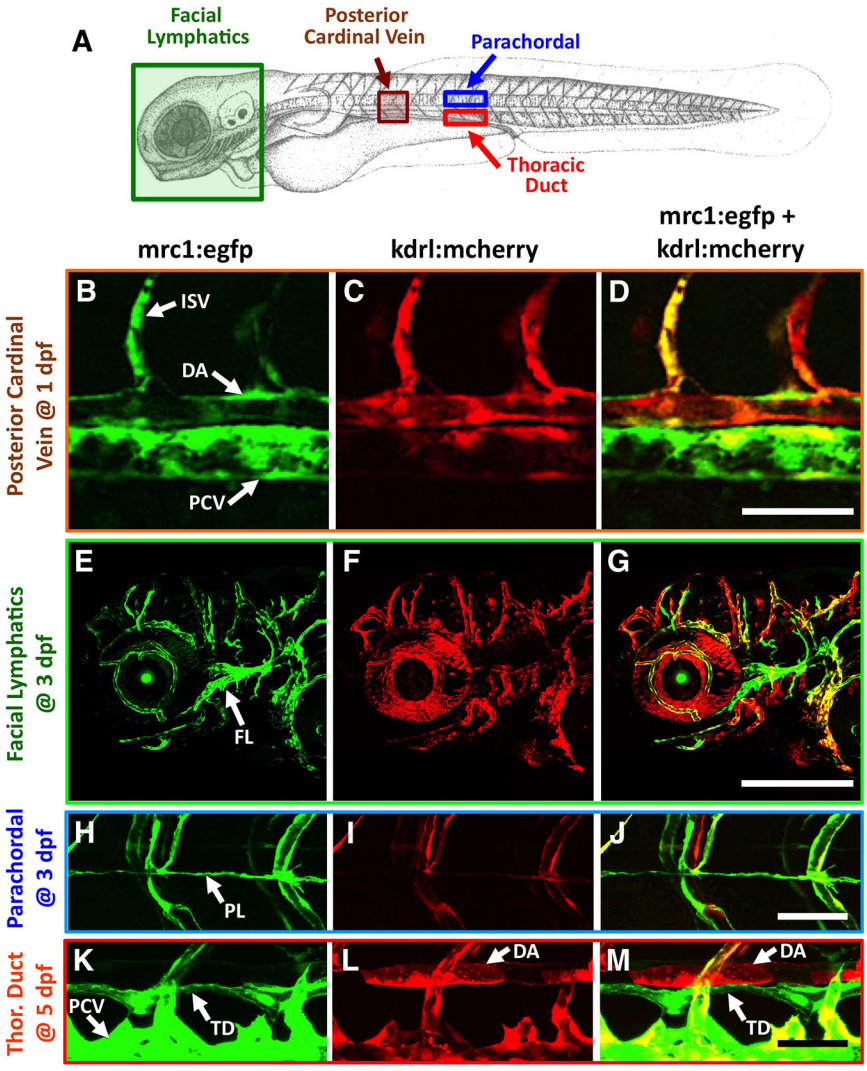

Fig. 3. *Tg(mrc1a:egfp)*^{y251} transgenic zebrafish express EGFP in veins and lymphatics. (A) Diagram with boxes indicating the approximate regions imaged in the confocal micrographs below. ('Parachordal' refers to parachordal lines.) (B-M) Confocal images of *mrc1a:egfp* fluorescence (B,E,H,K), *kdrl:mcherry* fluorescence (C,F,I,L), or both *mrc1a:egfp* and *kdrl:mcherry* fluorescence (D,G,J,M). (B-D) Ventral trunk at 1 dpf, showing the DA, PCV and ISV. (E-G) Head at 3 dpf, showing the FL. (H-J) Midtrunk at 3 dpf, showing the PL. (K-M) Ventral trunk at 5 dpf, showing the TD, PCV and DA. DA, dorsal aorta; FL, facial lymphatics; ISV, intersegmental vessel; PCV, posterior cardinal vein; PL, parachordal lines; TD, thoracic duct. All panels show lateral views, rostral to the left. Scale bars: 50 µm (B-D,H-M), 275 µm (E,F).

6-dpf *Tg(mrc1a:egfp)*^{y251}, *Tg(kdrl:mcherry)*^{y171} double-transgenic zebrafish, these developing CCLs are initially observed as shorter segments with multiple links to both the PCV and TD (Fig. 5A-C and Movie 5). Although many of the connections to the TD appear obviously patent, the links to the PCV do not, and microangiography of the blood vasculature does not result in obvious dye filling of the CCLs. At 6 dpf, the CCLs are weakly *kdrl:mcherry* positive (Fig. 5B). By 12 dpf, continuous CCL vessels run down the length of the trunk on either side of the pronephric duct. The CCLs are substantially enlarged by this stage and often wider than the TD, although the vessels appear somewhat flattened in profile (Fig. 5D-I and Movie 6). The CCLs are no longer *kdrl:mcherry* positive at this time (Fig. 5E). To confirm the lymphatic identity of the CCLs and other later-developing vessels described below, we crossed *Tg(mrc1a:egfp)*^{y251} to *Tg(lyve1:dsRed)*^{nz101} or *Tg(prox1aBAC:KalTA4-4xUAS-E1b:uncTagRFP)*^{nim5} and showed that the Mrc1-positive later-developing lymphatic vessels also co-express the lymphatic markers Lyve1 (Fig. S5) and Prox1 (Fig. S6). By 12 dpf, the links between the CCLs and PCV have mostly disappeared, but multiple enlarged connections to the TD are evident and dye filling of the CCLs from the TD is readily observed (Fig. S7).

In order to determine the origins of lymphatic endothelial progenitors contributing to the formation of the CCLs, we performed three independent sets of experiments. First, we obtained confocal images of the same *Tg(mrc1a:egfp)*^{y251}, *Tg(kdrl:mcherry)*^{y171} double-transgenic animal at 4, 4.5, 5 and 6 dpf to capture CCL development. Starting at 4 dpf, sprouts bud out from the ventral side of the PCV and extend rostrally and caudally, interconnecting to form a continuous CCL (Fig. S8). Next, we carried out overnight time-lapse imaging on a *Tg(mrc1a:egfp)*^{y251}, *Tg(kdrl:mcherry)*^{y171} double-transgenic zebrafish at 3-4 dpf to monitor the initial development of the CCL (Movie 7). As expected, sprouts giving rise to the CCL emerged from the ventral PCV. The two sets of experiments described above (Fig. S8 and Movie 7) and the connections between the CCL and PCV at 6 dpf (Fig. 5C) suggested that the PCV is a major source of CCL progenitors. To confirm this, we used *Tg(fliep:gal4ff)*^{ubs4}, *Tg(UAS:Kaede)* double-transgenic animals to photoconvert Kaede protein from green to red fluorescence in the PCV at 3 dpf before CCL formation initiates (Fig. 5J,K), followed by imaging at 6 dpf after the CCL is largely formed (Fig. 5L). Six of the 12 animals imaged formed a CCL segment adjacent to photoconverted portions of the PCV during the course of the experiment, and in all six of these animals the part of the CCL adjacent to the photoconverted PCV mainly expressed red Kaede protein (Fig. 5L). In the other six animals the CCL failed to assemble adjacent to the photoconverted PCV by 6 dpf (although it did assemble adjacent to

Development (2017) 144, 2070-2081 doi:10.1242/dev.145755

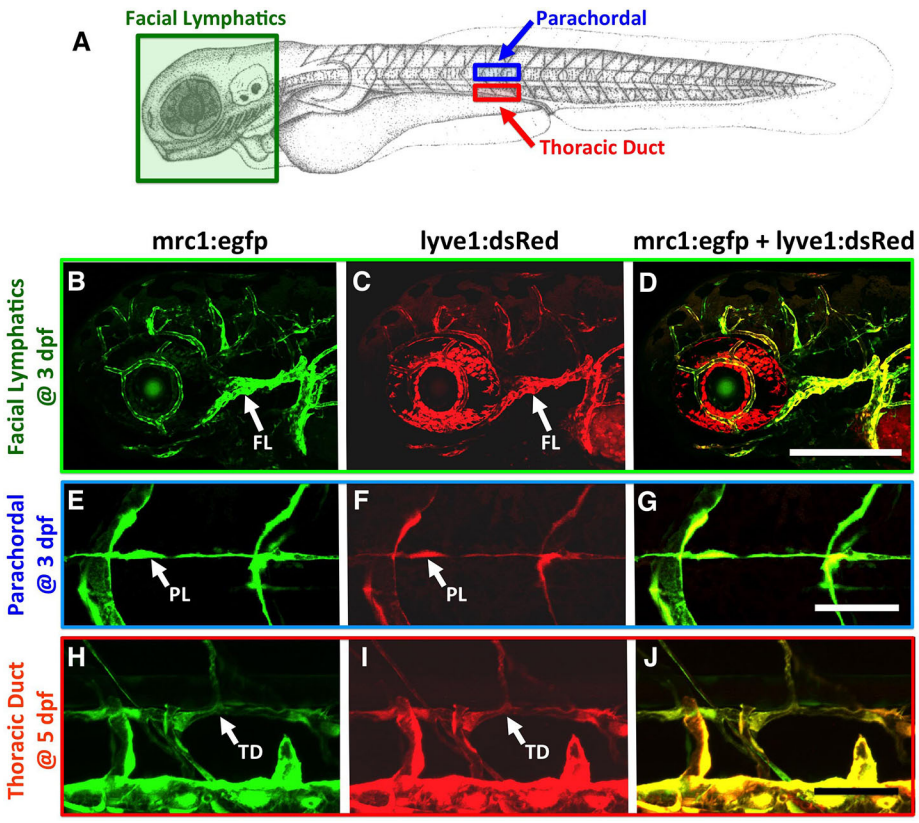

Fig. 4. Comparative expression patterns of *Tg (mrc1a:egfp)^{y251}* and *Tg(lyve1:dsRed)^{nz101}* transgenes. (A) Diagram with boxes indicating the approximate regions imaged in the confocal micrographs below. ('Parachordal' refers to parachordal lines.) (B-J) Confocal images of *mrc1a:egfp* fluorescence (B,E,H), *lyve1:dsRed* fluorescence (C,F,I), or both *mrc1a:egfp* and *lyve1:dsRed* fluorescence (D,G,J) in *Tg(mrc1a:egfp)^{y251}*, *Tg(lyve1:dsRed)^{nz101}* double-transgenic animals. (B-D) Head at 3 dpf, showing the FL. The red signal around the eye (C) is iridophore autofluorescence. (E-G) Midtrunk at 3 dpf, showing the PL. (H-J) Ventral trunk at 5 dpf, showing the TD. All panels show lateral views, rostral to the left. Scale bars: 275 µm (A-D), 50 µm (E-J).

nonphotoconverted portions of the PCV), suggesting that proper CCL development can be inhibited by exposure to the confocal laser used for photoconversion. We have noted in other experiments that the growth of lymphatic vessels is particularly sensitive to excess exposure to laser illumination (H.M.J., unpublished). Together, these results show that cells from the PCV are major contributors to CCL formation (Fig. 5M).

Formation of the superficial lymphatics

By 13 dpf, a complex network of superficial lymphatic vessels has formed near the surface of the trunk in juvenile zebrafish (Fig. 6A,B). This network of lymphatic vessels consists of a superficial lateral lymphatic (LL) vessel running longitudinally along the superficial horizontal myoseptum of the trunk and superficial intersegmental lymphatics (SILs) that extend dorsally and ventrally from the LL along vertical myosepta (Fig. 6A,B, Fig. S4 and Movie 8). All of these *mrc1a:egfp*-positive lymphatic vessels are closely apposed to *kdrl:mcherry*-positive lateral (LV) and superficial intersegmental (SIV) blood vessels, as visualized in *Tg(mrc1a:egfp)^{y251}*, *Tg(kdrl:mcherry)^{y171}* double-transgenic animals (Fig. 6C,D,E and Movie 8). The identity of the *kdrl:mcherry*-positive blood vessels can be verified by their labeling via intracardiac (intravascular) injection of Qdot705 quantum dots (Fig. 6F and Fig. S9A). Similarly, the identity of *mrc1a:egfp*-positive vessels as lymphatics is verified by both the absence of Qdot705 labeling after intracardiac injection (Fig. 6F), and by effective filling of these vessels following intramuscular injection of Qdot705 quantum dots into the tail and uptake into the lymphatic vasculature (Fig. 6G and Fig. S9B). Expression of lymphatic markers Lyve1 and Prox1 on these vessels also confirms their lymphatic identity (Figs S5 and S6).

The LL forms along the superficial horizontal myoseptum. It assembles at or very close to the former location of the PL, the cords of lymphatic progenitors that form earlier in development at ~3 dpf but then largely disassemble, contributing cells to the deep intersegmental lymphatics that run along intersegmental arteries and from there to the TD and dorsal longitudinal lymphatic [also known as the dorsal lymphatic (DL)] vessel [see Cha et al. (2012) for a detailed explanation]. The LL forms from *mrc1a:egfp*-positive sprouts that emerge from the deep intersegmental lymphatics at the level of the myotomal boundaries at ~5-7 dpf, growing laterally and then branching rostrally and caudally near the lateral surfaces of the trunk (Fig. 6H-K, Fig. S9C-L and Movie 9). Interestingly, LL sprouts emerge alongside *kdrl:mcherry*-positive blood vessel sprouts that are also growing laterally from ISVs, and these branch rostrally and caudally at approximately the same time or slightly earlier than LL sprouts (Fig. S9C-L). These blood vessels branch and form a continuous vessel at a more medial position than the developing LL, which is found at a more lateral/superficial position (Fig. S9K,L). By 9 dpf, branching LL sprouts have interconnected to form a continuous or largely continuous LL (Fig. 6L).

The dorsal (dSIL) and ventral (vSIL) superficial intersegmental lymphatics (Fig. 6B) sprout from the LL with variable timing between 4 and 13 dpf, extending along the myotomal boundaries (Fig. 6B,L-Q and Movie 10). The growth of *mrc1a:egfp*-positive SILs most often appears to lag slightly behind that of adjacent *kdrl:mcherry*-positive superficial intersegmental blood vessels, although they are also frequently observed paralleling or even preceding the growth of the blood vessels (Fig. 6R,S), suggesting that the blood and lymphatic superficial ISVs are most likely independently finding their paths along the myotomal septa as they grow and extend dorsally and ventrally. At 13 dpf, the LL and SILs all remain closely paired with adjacent blood vessels, which are invariably at a slightly deeper position than the more superficial lymphatic vessels (Fig. S9M-Q and Movie 11). The superficially located SILs observed at 13 dpf are distinct from deeper intercostal lymphatic

Development (2017) 144, 2070-2081 doi:10.1242/dev.145755

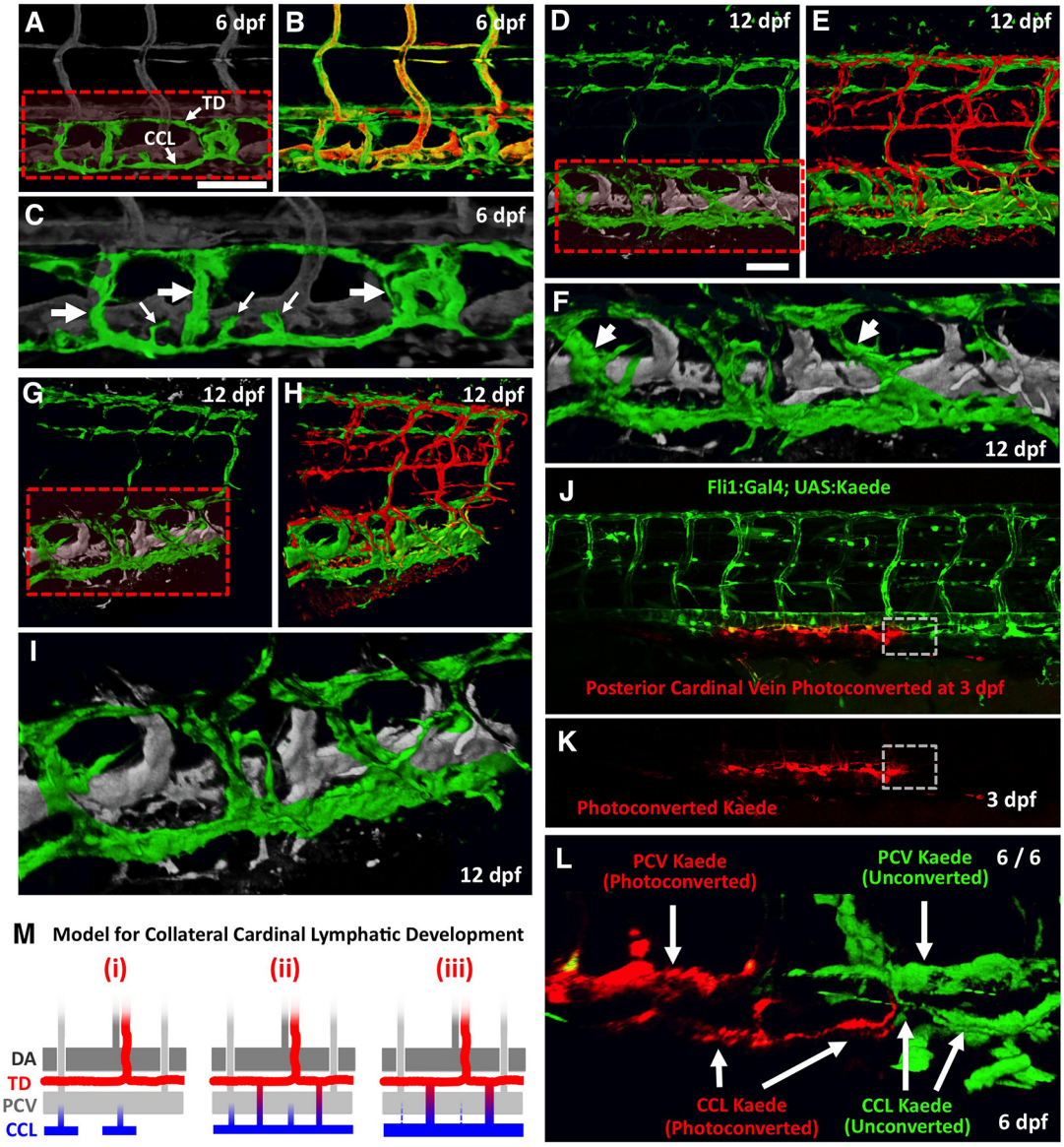

Fig. 5. Formation of the CCLs. (A-C) Confocal image reconstructions of the ventral trunk of a 6-dpf *Tg(mrc1a:egfp)*^{y251}*, Tg(kdrl:mcherry)*^{y171} double-transgenic animal, showing (A) the TD and CCL highlighted in green, with all other blood and lymphatic vessels in gray; (B) same image data as in A but unmanipulated, with *mrc1a:egfp* fluorescence in green and *kdrl:mcherry* fluorescence in red; and (C) magnified image of the boxed region from A. Large arrows (C) indicate connections between the CCL and TD; small arrows indicate links between the CCL and PCV. (D-I) Confocal image reconstructions of the ventral trunk of a 12-dpf *Tg(mrc1a:egfp)*^{y251}*, Tg(kdrl:mcherry)*^{y171} double-transgenic animal, showing (D,G) the TD and CCL highlighted in green, with all other blood and lymphatic vessels in gray; (E,H) same image data as in D and G but unmanipulated, with *mrc1a:egfp* fluorescence in green and *kdrl:mcherry* fluorescence in red; and (F,I) magnified images of the boxed regions from D and G, respectively. Arrows (F) indicate large connections between the CCL and TD. (J) Green-to-red photoconversion of the PCV in a 3-dpf *Tg(fliep:gal4ff)* ^{ubs4}*, Tg(UAS:Kaede)* double-transgenic zebrafish, showing a green and red confocal fluorescence image immediately after photoconversion. (I) Red confocal fluorescence image showing the photoconverted PCV at 3 dpf. (L) Confocal image of green and red fluorescence in the ventral trunk at 6 dpf. The boundary of the photoconverted (red) and unconverted (green) area of the PCV and CCL is shown. Successful CCL formation occurred in six of 12 experiments; in all six (6/6) the part of the CCL adjacent to the photoconverted PCV expressed red Kaede protein. (M) Model for CCL formation in the ventral trunk. (i) Sprouting of CCL from the PCV; (ii) anastomosis of CCL and connection to the TD; (iii) enlargement of CCL and beginning of its disconnection from the PCV. All panels show lateral views, rostral to the left. Scale bars: 100 µm.

vessels (ICLVs) that are evident at each myotomal segment boundary at later stages of development. At 25 dpf, these deep ICLVs are observed immediately adjacent to each rib bone (Fig. S9R,S). Although the deep location of the ICLVs makes them difficult to image at this stage by confocal microscopy (Fig. S9T), SILs are readily imaged at all stages of development and even in adults. The lymphatic identities of both the SILs and ICLVs can be confirmed by the filling of these vessels by drainage of subcutaneously injected Qdot705 quantum dots (Fig. S9U).

Examination of blood flow through the adjacent blood vessels in 20 separate 19-dpf *Tg(mrc1a:egfp)*^{y251}*, Tg(kdrl:mcherry)*^{y171}*, Tg(gata1:dsRed)*^{sd2} triple-transgenic zebrafish (Fig. S10 and Movie 12; lymphatics, green; blood vessels, red; blood cells, red) showed that the direction of flow in blood vessels adjacent to the SILs was random, with approximately equal numbers flowing in each direction, suggesting that SILs do not preferentially form adjacent to either arteries or veins (Fig. S10 and Movie 12). Since lymphatic vessels are used as a conduit for immune cell trafficking,

Development (2017) 144, 2070-2081 doi:10.1242/dev.145755

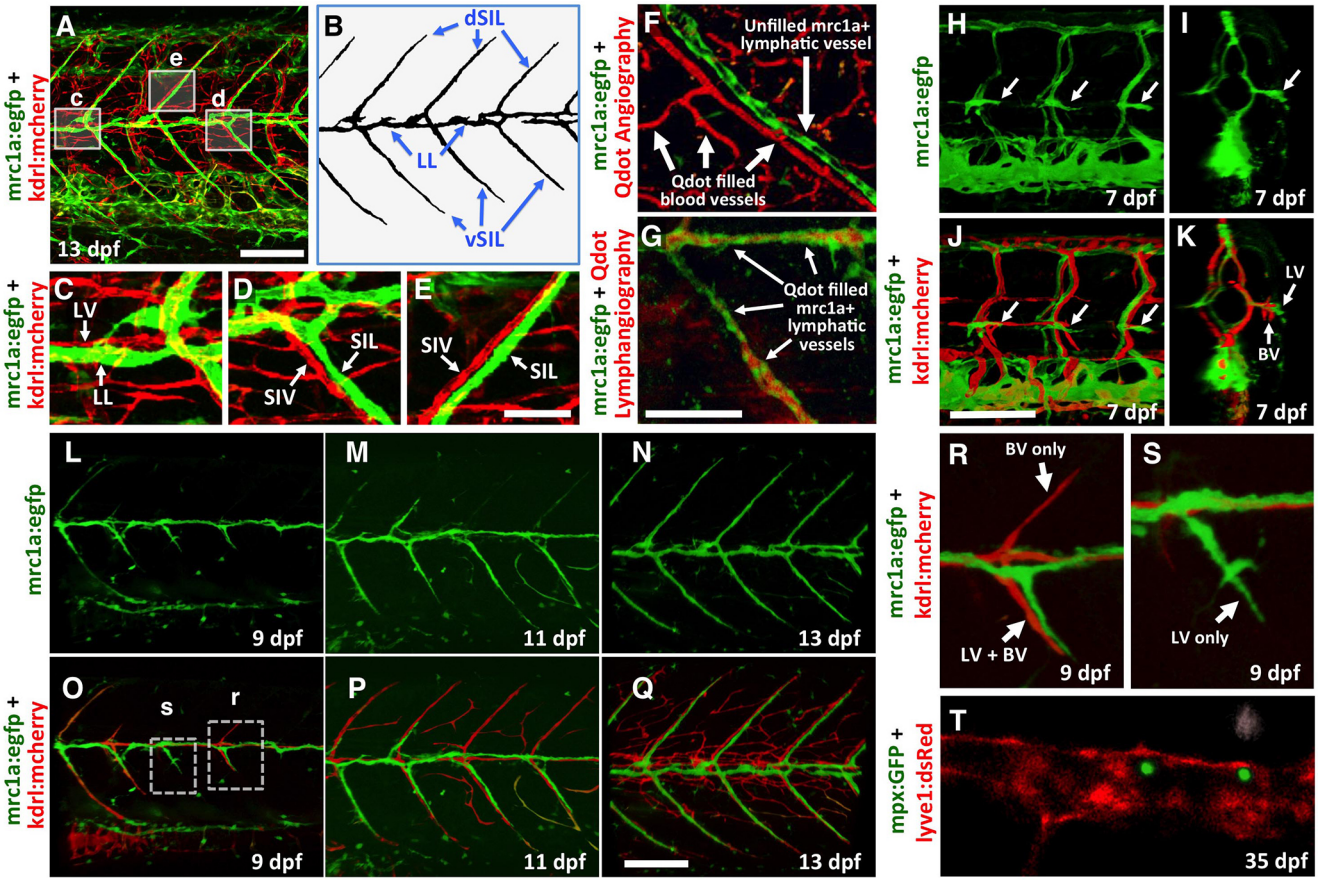

Fig. 6. Formation of the SILs. (A) Confocal micrograph of the midtrunk of a 13-dpf *Tg(mrc1a:egfp)*^{y251}, *Tg(kdrl:mcherry)*^{y171} double-transgenic zebrafish (lymphatics, green; blood vessels, red). (B) Schematic showing the superficial lymphatic vessels imaged in A. (C-E) Magnified portions of the indicated regions (c, d and e) in A, showing *mrc1a:egfp*-positive lymphatic vessels aligned with adjacent *kdrl:mcherry*-positive blood vessels. (F) Confocal micrograph of the superficial vessels in the midtrunk of a 28-dpf *Tg(mrc1a:egfp)*^{y251} transgenic zebrafish after intracardiac injection of Qdot705 quantum dots to label the blood vascular system (lymphatics, green; blood vessels labeled by intravascular Qdot705, red). See Fig. S9A for a lower-magnification view. (G) Confocal micrograph of superficial vessels in the midtrunk of a 28-dpf *Tg(mrc1a:egfp)*^{y251} transgenic zebrafish after intramuscular injection of Qdot705 quantum dots into the tail to label the trunk lymphatic system (lymphatics, green; intralymphatic Qdot705, red). See Fig. S9B for a lower-magnification view. (H-K) Confocal micrographs of *mrc1a:egfp* (green, H-K) and *kdrl:mcherry* (red, J,K) fluorescence in the midtrunk of a 7-dpf *Tg(mrc1a:egfp)*^{y251}, *Tg(kdrl:mcherry)*^{y171} double-transgenic zebrafish. Images show lateral (H,J) and transverse (I,K) views of the same confocal image data set. Arrows indicate growing lymphatic sprouts from the deep intersegmental lymphatics. (K) The positions of the tips of the lateral lymphatic vessel (LLV) and lateral blood vessel (LBV) sprouts are shown, with the LLV tips extending further laterally. (L-N) Confocal micrographs of superficial *mrc1a:egfp* fluorescence in the midtrunk of 9-dpf (L), 11-dpf (M) and 13-dpf (N) *Tg(mrc1a:egfp)*^{y251}, *Tg(kdrl:mcherry)*^{y171} double-transgenic zebrafish. (O-Q) Confocal micrographs of superficial *mrc1a:egfp* and *kdrl:mcherry* fluorescence in the same animals and same fields imaged in L-N. (R,S) Magnified images of the boxes (r and s) in O, respectively, showing *kdrl:mcherry*-positive blood vessel (BV) sprouts and *mrc1a:egfp*-positive lymphatic vessel (LV) sprouts that are either extending in the absence of the other vessel type or side by side. (T) Confocal image of *mpx:GFP*-positive neutrophils inside the superficial LLV in *Tg(lyve1:dsRed)*^{nz101}, *Tg(mpx:GFP)*^{i114} double-transgenic 35-dpf zebrafish (lymphatics, red; neutrophils, green). The mpx:GFP signals outside the lymphatics are pseudocolored in grayscale. All panels show lateral views, rostral to the left. Scale bars: 150 µm (A,F-Q), 40 µm (C-E).

we used *Tg(mpx:GFP)*^{i114} (for neutrophils) and *Tg(lck:GFP)* (for lymphocytes) to track movements of immune cells. At 15 dpf, we observed lymphocytes in lymphatic vessels (Fig. S11 and Movie 13); at 35 dpf, we were able to find neutrophils in the FL as well as in the LL (Fig. 6T and Movie 14). By 13 dpf, many of the connections of the LL back to the deep intersegmental lymphatics from which they sprouted have disappeared, along with the deep intersegmental lymphatics themselves (Movie 8).

Absence of smooth muscle or pericyte coverage is a feature of most smaller-caliber mammalian lymphatic vessels, so we examined whether trunk lymphatic vessels in later-stage larval zebrafish possess pericytes using a double-transgenic line. We imaged 12-dpf *TgBAC(pdgfrb:mCitrine), Tg(lyve1:dsRed)*^{nz101} double-transgenic animals but failed to observe *pdgfrb*-positive pericytes lining either major deep lymphatic vessels, such as the TD, or smaller-caliber superficial lymphatic vessels, although abundant pericyte coverage was noted on small-caliber blood vessels immediately adjacent to these lymphatic vessels (Fig. S12 and Movie 15). Our findings do not rule out the possibility that pericytes might be associated with zebrafish lymphatic vessels at even later stages of development or in adults, perhaps on larger-caliber collecting lymphatics (as in mammals).

Formation of the SL

Examination of vascular structures in 13-dpf juvenile *Tg(mrc1a:egfp)*^{y251}, *Tg(kdrl:mcherry)*^{y171} double-transgenic animals also revealed the presence of a novel deep lymphatic vessel, the SL (Fig. 7A, Fig. S4, Movie 8 and 16). This vessel forms at the trunk midline immediately dorsal to the developing spinal cord (SC) (Fig. 7B, Movie 8 and 16). The SL assembles from sprouts that emerge from the DL vessel, generally near the myotomal boundaries, at ∼9 dpf. These sprouts grow ventrally until they

Development (2017) 144, 2070-2081 doi:10.1242/dev.145755

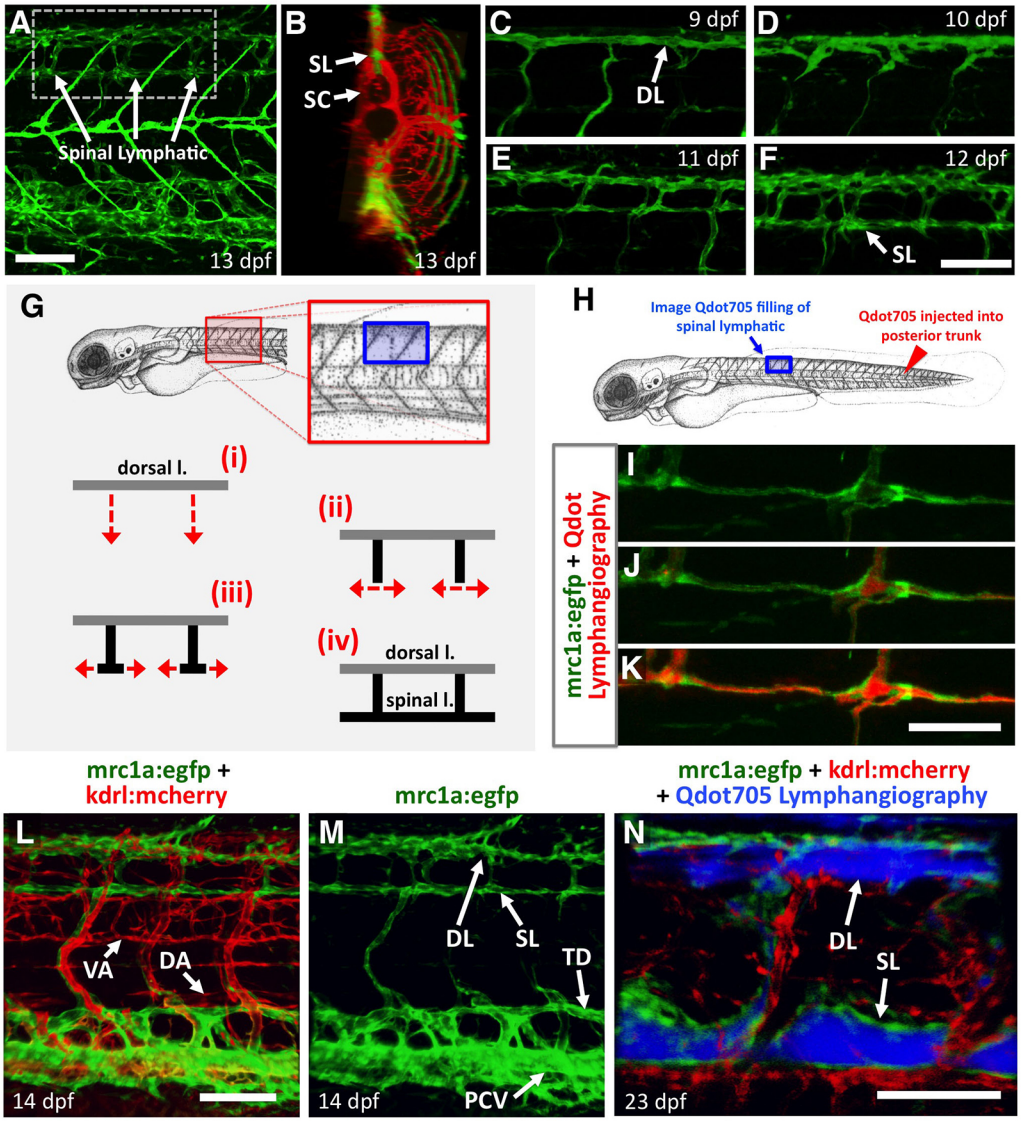

Fig. 7. Formation of the SL. (A) Confocal micrograph of *mrc1a:egfp* fluorescence in the midtrunk of a 13-dpf *Tg(mrc1a:egfp)*^{y251}*, Tg(kdrl:mcherry)*^{y171} double-transgenic zebrafish (lateral view). Dashed box indicates the approximate location of the magnified images in C-F. (B) Confocal micrograph of *mrc1a:egfp* and *kdrl:mcherry* fluorescence in the midtrunk of the same 13-dpf *Tg(mrc1a:egfp)*^{y251}*, Tg(kdrl:mcherry)*^{y171} double-transgenic zebrafish in A. Image shows transverse view, with the positions of the SC and SL indicated. (C-F) Confocal micrograph of *mrc1a:egfp* fluorescence in the dorsal midtrunk of *Tg(mrc1a:egfp)*^{y251}*, Tg(kdrl:mcherry)*^{y171} double-transgenic zebrafish at the indicated stages (lateral views). (G) The process of SL formation from DL-derived sprouts. (i) Sprouting of SL from DL and ventral growth; (ii) initial rostral and caudal growth of SL; (iii) rostral and caudal extension of SL; (iv) complete formation of SL. (H) Diagram showing the approximate location of intramuscular injection of Qdot705 quantum dots (red) and the approximate region further rostrally in the trunk in I-K (blue box). (I-K) Confocal micrograph of *mrc1a:egfp* fluorescence (green) and Qdot705 fluorescence (red) in the dorsal midtrunk of 12-dpf *Tg(mrc1a:egfp)*^{y251} transgenic zebrafish subjected to intramuscular injection of Qdot705 quantum dots in the tail, imaged at the start (I), middle (J) and end (K) of Movie 17, over a total elapsed time of 4 min 34 s. (L,M) Confocal micrographs of *mrc1a:egfp* (L,M) and *kdrl:mcherry* (L) fluorescence in the midtrunk of a 14-dpf *Tg(mrc1a:egfp)*^{y251}*, Tg(kdrl:mcherry)*^{y171} double-transgenic zebrafish. (N) Confocal micrograph of *mrc1a:egfp* fluorescence (green), *kdrl:mcherry* fluorescence (red) and Qdot705 fluorescence (blue) in the dorsal midtrunk of 23-dpf *Tg(mrc1a:egfp)*^{y251}*, Tg(kdrl:mcherry)*^{y171} double-transgenic zebrafish subjected to intramuscular injection of Qdot705 quantum dots in the tail. (A,C-N) Lateral views, rostral to the left; (B) transverse view, dorsal up and right to the right. DA, dorsal aorta; DL, dorsal lymphatic; PCV, posterior cardinal vein; SC, spinal cord; SL, spinal lymphatic; TD, thoracic duct; VA, vertebral artery. Scale bars: 150 µm (A-F,L-N), 50 µm (I-K).

reach the level of the dorsal roof of the SC, and then they branch rostrally and caudally, interconnecting to form a continuous SL (Fig. 7C-G and Movie 16).

The identity of this new vessel as a bona fide lymphatic vessel is verified by effective filling of this vessel following intramuscular injection of Qdot705 quantum dots into the tail (Fig. 7H-K and Movie 17), as well as by absence of filling after microangiography to visualize the blood vascular network (data not shown). Although the SL appears comparable to or smaller than the DL at earlier stages of development (Fig. 7L,M), at later stages the SL enlarges beyond the size of the DL, becoming one of the largest trunk highways for lymph drainage (Fig. 7N). Like the superficial lateral and intersegmental lymphatic vessels, the SL also appears to develop adjacent to blood vessel tracts (Fig. 7L,M and Movie 16).

DISCUSSION

Here, we provide the first report of a new transgenic line using the *mrc1a* promoter to visualize and study the primitive venous lymphatic vasculature in the zebrafish. We show that this *Tg(mrc1a:egfp)*^{y251} transgene is expressed in previously described

Development (2017) 144, 2070-2081 doi:10.1242/dev.145755

zebrafish lymphatic vessels and lymphatic vessel progenitors including the PL, TD, deep intersegmental lymphatics and DL (Bussmann et al., 2010; Cha et al., 2012; Okuda et al., 2012; Yaniv et al., 2006). We demonstrate that the vascular expression pattern of this new *Tg(mrc1a:egfp)*^{y251} line is similar to that of the previously reported *Tg(lyve1:dsRed)*^{nz101} line (Okuda et al., 2012). We also note *Tg(mrc1a:egfp)*^{y251} expression in the maternal germline, where Mrc1a could potentially be involved in the fertilization process (Benoff et al., 1993; Dong et al., 2004), hormone recognition and uptake, or clearance of glycoproteins produced from pathogenic microbes coated with mannose structures (Lee et al., 2002; Taylor et al., 2005a).

Residual maternally derived ubiquitous EGFP is largely gone by 48 hpf, and it can easily be eliminated entirely by examining transgenic embryos and larvae obtained by crossing *Tg(mrc1a:egfp)*^{y251} male carriers to wild-type female fish. *Tg(mrc1a:egfp)*^{y251} is strongly expressed in heterozygotes, and there is no early embryonic expression if the transgene is only passed through the male germline (Fig. S1). The *mrc1a* promoter also expresses many other transgenes strongly, and the Tol2 promoter-containing construct provides a robust and easily used vector for driving primitive venous and lymphatic expression. We have used this construct to generate a variety of transgenic lines, and it has proven to be uniformly efficient for germline transgenesis (data not shown).

We have used the *Tg(mrc1a:egfp)*^{y251} transgenic line to study the development of the zebrafish lymphatic vascular network. Published descriptions of the formation of the lymphatic system in the zebrafish have been largely confined to the first 5 or 6 days of development (Fig. 8A-D) (Astin et al., 2014; Cha et al., 2012; Hogan et al., 2009; Isogai et al., 2009; Koltowska et al., 2015; Kuchler et al., 2006; Mulligan and Weinstein, 2014; Nicenboim et al., 2015; Okuda et al., 2012; van Impel et al., 2014). This initial network forms from sprouts that emerge from the cardinal vein at ~1.5 dpf. By 3 dpf, these contribute to the assembly of the PL, early transient progenitor structures that give rise to trunk lymphatic vessels (Cha et al., 2012; Yaniv et al., 2006). Lymphatic sprouts from the PL grow dorsally and ventrally along intersegmental arteries from 3-5 dpf, and then branch and anastomose to give rise to the TD (just below the DA) and DL (just below the dorsal longitudinal anastomotic vessel).

We have now extended these findings to elucidate the assembly of other major superficial and deep lymphatic vessels forming in the trunk (Fig. 8E-H). Similar to earlier-forming lymphatic vessels, these later larval trunk lymphatics also develop in a highly

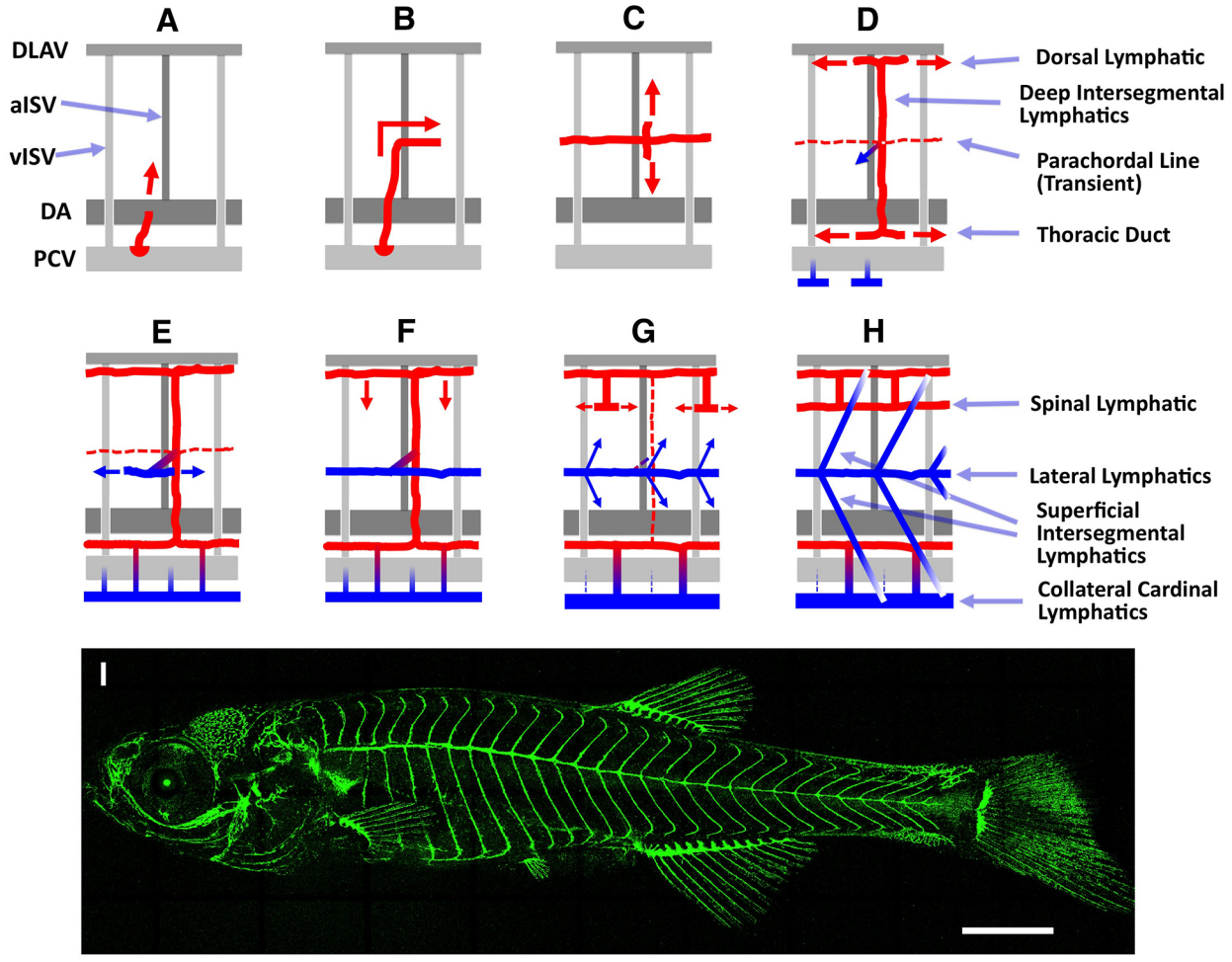

Fig. 8. Trunk lymphatic network formation. (A-D) Model for formation of the early trunk lymphatic vascular network from 1-5 dpf [modified from Cha et al. (2012)]. Major arteries and veins are shown in dark gray and light gray, respectively; the developing lymphatics are shown in red. Sprouts for the lateral lymphatics and CCLs are shown in blue. (E-H) Model for formation of the later larval lymphatic vascular network from ~6-14 dpf. The developing lymphatics are shown in red (deep lymphatics) and blue (superficial lymphatics). Detailed explanations of later larval lymphatic development are provided in the main text. (I) Composite-tiled confocal image of *mrc1a:egfp*-positive superficial lymphatics in a 19-dpf *Tg(mrc1a:egfp)*^{y251} transgenic zebrafish. Scale bar: 1 mm.

Development (2017) 144, 2070-2081 doi:10.1242/dev.145755

stereotyped and patterned fashion. In the ventral trunk, the TD is joined by an additional pair of lymphatic vessels, the CCLs. The CCLs form slightly ventrolateral to the PCV, beginning as shorter segments that assemble into complete lines running bilaterally along the ventral trunk from ∼5-12 dpf. Using confocal time-series imaging, confocal time-lapse imaging and photoconversion experiments, we have shown that CCL progenitors emerge from the PCV (Fig. 5J-M, Fig. 8D, Fig. S8 and Movie 7).

Beginning at ∼5-7 dpf, sprouts emerge laterally from the deep intersegmental lymphatics at the level of the horizontal myoseptum (Fig. 8D). These sprouts grow laterally until they reach the surface of the animal, where they branch rostrally and caudally along the horizontal myoseptum just below the skin (Fig. 8E) and then anastomose to form a continuous LL by ∼9 dpf (Fig. 8F). As the LL becomes continuous, sprouts of SILs begin to branch dorsally and ventrally from the LL and grow along each vertical myoseptal boundary (Fig. 8G). These sprouts grow to form a complete SIL network that extends across virtually the entire dorsal-ventral span of the superficial surface of the trunk (Fig. 8H,I). The presence of some of these superficial vessels in later-stage zebrafish was noted in a previous report (Okuda et al., 2012), especially the more ventral SILs, although the authors misidentified these SILs as ICLVs. The ICLVs are in fact a distinct and separate set of even later-forming lymphatic vessels that assemble deep in the trunk immediately adjacent to each rib (Fig. S9R-U). ICLVs only form on the ventral side of the fish juxtaposed to the ribs, whereas the superficial SILs grow both ventrally and dorsally. Our descriptions of these vessels use the teleost nomenclature of Dr Otto Kampmeier and other classical authors (Kampmeier, 1969), as well as nomenclature used previously in zebrafish (Isogai et al., 2009). The superficial lymphatic network will be of great interest to investigators focusing on later-stage lymphatics and their function. Imaging vessels in later-stage larval or juvenile zebrafish is usually very technically challenging owing to the depth and thickness of the tissues, but since the superficial lymphatic network is extremely close to the surface of the animal it is feasible to acquire high-resolution images to capture events such as trafficking of immune cells in these lymphatics, even at 35 dpf (Fig. 6T and Movie 14).

Interestingly, much or all of the superficial lymphatic network is closely paralleled by nearby blood vessels (Fig. S9). Our observations suggest that the growth of superficial lymphatic vessels and blood vessels is likely to be guided independently, not by one vessel type tracking along the other type, since we frequently observe lymphatic sprouts appearing to precede adjacent blood vessels and vice-versa (Fig. 6R,S). This suggests that these blood and lymphatic vessels might each be guided by cues from nearby tissues, potentially similar sets of external guidance cues. Although these cues remain to be elucidated, the zebrafish has proven to be a useful experimental model for uncovering molecular mechanisms directing the guidance and patterning of vessels (Cha et al., 2012; Torres-Vázquez et al., 2004).

The SL assembles from sprouts that grow ventrally from the DL, and through the stages we have examined appears to remain connected to it (Fig. 7C-G and Fig. 8F-H). Although this vessel is initially smaller and thinner, over time it enlarges beyond the size of the DL to become one of the major lymphatic drainage highways for the trunk. The SL also has a few connections to the deep intersegmental lymphatics, at least at initial stages (e.g. Fig. 7E), but most of these connections are lost as the deep ISVs disappear. Similar to the early PL, which serve as transient structures giving rise to the 5-dpf deep intersegmental lymphatics, TD and DL, the deep ISVs of the early larva also appear to be mostly transient, disappearing after the lateral sprouts have emerged to initiate growth and assembly of the superficial lymphatic system (Fig. 8D-H). The lateral sprouts are also absent at later stages, leaving the superficial and deep lymphatic vessels largely separated from each other. It remains to be determined whether some of these connections and vessel tracts reform in the adult fish.

In this study, we have introduced a new transgenic zebrafish model using the *mrc1a* promoter to visualize the development of lymphatic vessels. The robust expression of EGFP in *Tg(mrc1a:egfp)*^{y251} makes this a very useful line for imaging even the smallest lymphatic vessels and for documenting later-developing lymphatic vessels in deep tissues (Fig. 8I). Building on previous reports from our laboratory and other groups documenting mechanisms of lymphatic vessel assembly in the zebrafish during the first 5 days of development, our findings document the assembly of a series of well-conserved lymphatic structures that feature prominently in the adult lymphatic system. This study and our new transgenic model provide important new resources for further genetic and experimental investigation of lymphatic development in the zebrafish.

MATERIALS AND METHODS

Zebrafish

Zebrafish were maintained and zebrafish experiments were performed according to standard protocols (Westerfield, 2000). The research protocols were reviewed and approved by the Eunice Kennedy Shriver National Institute of Child Health and Human Development (NICHD) Animal Care and Use Committee at the NIH. All animal studies were conducted in accordance with the Guide for the Care and Use of Laboratory Animals in an Association for Assessment and Accreditation of Laboratory Animal Care (AAALAC)-accredited facility.

Whole-mount RNA *in situ* hybridization (ISH)

Digoxigenin (DIG)-labeled antisense riboprobes for *mrc1a*, *dll4* and *lyve1* were generated using a DIG RNA Labeling Kit (Roche). ISH was performed as described (Swift et al., 2014). BM Purple or nitro blue tetrazolium (NBT)/5-bromo-4-chloro-3-indoylphosphate (BCIP) was used for DIG-labeled probes.

Generation of the expression construct and transgenic line

The expression construct was generated using Tol2kit components with Gateway Technology (Kwan et al., 2007). Briefly, a 1.9 kb genomic sequence upstream from the transcription start site, combined with a 0.3 kb enhancer sequence located in intron 19 of the *mrc1a* gene, was cloned into pDONR vector using BP Clonase (Thermo Fisher Scientific). The enhancer region was selected based on high conservation between *mrc1a* and *mrc1b* noncoding regions. LR Clonase II (Thermo Fisher Scientific) was used to generate an *mrc1a:egfp* expression construct. The DNA construct was microinjected into the blastomere of one-cell stage zebrafish embryos. *Tg(lyve1:dsRed)*^{nz101}, *Tg(prox1aBAC:KalTA4-4xUAS-E1b:uncTagRFP)*^{nim5}, *Tg(gata1:dsRed)*^{sd2}, *Tg(lck:GFP)*, *Tg(mpx:GFP)*^{i114}, *Tg(fliep:gal4ff)*^{ubs4}, *Tg(UAS:Kaede)* and *TgBAC(pdgfrb:mCitrine)* were obtained from previous studies (Hatta et al., 2006; Langenau et al., 2004; Okuda et al., 2012; Renshaw et al., 2006; Totong et al., 2011; Traver et al., 2003; van Impel et al., 2014; Vanhollebeke et al., 2015). For the experiments performed using larvae older than 7 dpf, transgenics were crossed to *casper* (*nacre*$^{-/-}$, *roy*$^{-/-}$) background to avoid pigmentation (White et al., 2008).

Quantum dot injection

Qdot705 (Thermo Fisher Scientific) injections were performed as described (Yaniv et al., 2006). Undiluted Qdot705 was intramuscularly injected (for lymphatic drainage) or directly injected into the heart or caudal vein (for microangiography) using a filamented glass needle.

Kaede photoconversion

Green Kaede-positive 3-dpf embryos with *Tg(fliep:gal4ff)*^{ubs4}, *Tg(UAS:Kaede)* double-transgenic expression were mounted laterally in 1% low

Development (2017) 144, 2070-2081 doi:10.1242/dev.145755

melting point agarose. A portion of the PCV was exposed to a UV laser at 20 µs/pixel scanning rate on a FluoView 1000 (Olympus) microscope. After photoconversion, embryos were removed from agarose and placed in blue water and raised to 6 dpf at 28.5°C, when red Kaede expression was imaged using confocal microscopy.

Imaging methods

Embryos were anesthetized using 1× tricaine and mounted in 0.8-1.5% low melting point agarose or 5% methylcellulose dissolved in blue water and mounted on a depression slide. Confocal fluorescence imaging was performed using a FluoView 1000 (Olympus) or LSM 880 (Zeiss) microscope, and multiphoton laser scanning microscopy was performed using TCS SP5II (Leica). The 3D reconstructions were performed using Volocity 6.3 (PerkinElmer) and Imaris 7.4 (Bitplane) software.

Acknowledgements

We thank members of the B.M.W. laboratory for their critical comments on this manuscript.

Competing interests

The authors declare no competing or financial interests.

Author contributions

Conceptualization: H.M.J., S.I., B.M.W.; Methodology: H.M.J., D.C., M.R.S., S.I., B.M.W.; Validation: B.M.W.; Formal analysis: H.M.J., D.C., B.M.W.; Investigation: H.M.J., D.C., M.R.S., V.N.P., M.V.G., M.G.B., T.S.M., B.M.W.; Resources: M.R.S., M.V.G., B.M.W.; Data curation: H.M.J.; Writing - original draft: H.M.J., B.M.W.; Writing - review & editing: H.M.J., D.C., B.M.W.; Visualization: B.M.W.; Supervision: B.M.W.; Project administration: B.M.W.; Funding acquisition: B.M.W.

Funding

This work was supported by the intramural program of the Eunice Kennedy Shriver National Institute of Child Health and Human Development, National Institutes of Health (ZIA-HD008808 and ZIA-HD001011, to B.M.W.). Deposited in PMC for release after 12 months.

Supplementary information

Supplementary information available online at
http://dev.biologists.org/lookup/doi/10.1242/dev.145755.supplemental

References

Alitalo, K., Tammela, T. and Petrova, T. V. (2005). Lymphangiogenesis in development and human disease. *Nature* **438**, 946-953.

Astin, J. W., Haggerty, M. J. L., Okuda, K. S., Le Guen, L., Misa, J. P., Tromp, A., Hogan, B. M., Crosier, K. E. and Crosier, P. S. (2014). Vegfd can compensate for loss of Vegfc in zebrafish facial lymphatic sprouting. *Development* **141**, 2680-2690.

Baluk, P., Fuxe, J., Hashizume, H., Romano, T., Lashnits, E., Butz, S., Vestweber, D., Corada, M., Molendini, C., Dejana, E. et al. (2007). Functionally specialized junctions between endothelial cells of lymphatic vessels. *J. Exp. Med.* **204**, 2349-2362.

Banerji, S., Ni, J., Wang, S.-X., Clasper, S., Su, J., Tammi, R., Jones, M. and Jackson, D. G. (1999). LYVE-1, a new homologue of the CD44 glycoprotein, is a lymph-specific receptor for hyaluronan. *J. Cell Biol.* **144**, 789-801.

Benoff, S., Cooper, G. W., Hurley, I., Napolitano, B., Rosenfeld, D. L., Scholl, G. M. and Hershlag, A. (1993). Human sperm fertilizing potential in vitro is correlated with differential expression of a head-specific mannose-ligand receptor. *Fertil. Steril.* **59**, 854-862.

Bussmann, J., Bos, F. L., Urasaki, A., Kawakami, K., Duckers, H. J. and Schulte-Merker, S. (2010). Arteries provide essential guidance cues for lymphatic endothelial cells in the zebrafish trunk. *Development* **137**, 2653-2657.

Cha, Y. R., Fujita, M., Butler, M., Isogai, S., Kochhan, E., Siekmann, A. F. and Weinstein, B. M. (2012). Chemokine signaling directs trunk lymphatic network formation along the preexisting blood vasculature. *Dev. Cell* **22**, 824-836.

Dong, C.-H., Yang, S.-T., Yang, Z.-A., Zhang, L. and Gui, J.-F. (2004). A C-type lectin associated and translocated with cortical granules during oocyte maturation and egg fertilization in fish. *Dev. Biol.* **265**, 341-354.

Flores, M. V., Hall, C. J., Crosier, K. E. and Crosier, P. S. (2010). Visualization of embryonic lymphangiogenesis advances the use of the zebrafish model for research in cancer and lymphatic pathologies. *Dev. Dyn.* **239**, 2128-2135.

Fritz-Six, K. L., Dunworth, W. P., Li, M. and Caron, K. M. (2008). Adrenomedullin signaling is necessary for murine lymphatic vascular development. *J. Clin. Invest.* **118**, 40-50.

Hatta, K., Tsujii, H. and Omura, T. (2006). Cell tracking using a photoconvertible fluorescent protein. *Nat. Protoc.* **1**, 960-967.

Hermans, K., Claes, F., Vandevelde, W., Zheng, W., Geudens, I., Orsenigo, F., De Smet, F., Gjini, E., Anthonis, K., Ren, B. et al. (2010). Role of synectin in lymphatic development in zebrafish and frogs. *Blood* **116**, 3356-3366.

Hogan, B. M., Bos, F. L., Bussmann, J., Witte, M., Chi, N. C., Duckers, H. J. and Schulte-Merker, S. (2009). Ccbe1 is required for embryonic lymphangiogenesis and venous sprouting. *Nat. Genet.* **41**, 396-398.

Hong, Y.-K., Harvey, N., Noh, Y.-H., Schacht, V., Hirakawa, S., Detmar, M. and Oliver, G. (2002). Prox1 is a master control gene in the program specifying lymphatic endothelial cell fate. *Dev. Dyn.* **225**, 351-357.

Irjala, H., Johansson, E.-L., Grenman, R., Alanen, K., Salmi, M. and Jalkanen, S. (2001). Mannose receptor is a novel ligand for L-selectin and mediates lymphocyte binding to lymphatic endothelium. *J. Exp. Med.* **194**, 1033-1042.

Isogai, S., Hitomi, J., Yaniv, K. and Weinstein, B. M. (2009). Zebrafish as a new animal model to study lymphangiogenesis. *Anat. Sci. Int.* **84**, 102-111.

Jung, H. M., Isogai, S., Kamei, M., Castranova, D., Gore, A. V. and Weinstein, B. M. (2016). Imaging blood vessels and lymphatic vessels in the zebrafish. *Methods Cell Biol.* **133**, 69-103.

Kampmeier, O. F. (1969). *Evolution and Comparative Morphology of the Lymphatic System*. Springfield: Charles C. Thomas.

Koltowska, K., Lagendijk, A. K., Pichol-Thievend, C., Fischer, J. C., Francois, M., Ober, E. A., Yap, A. S. and Hogan, B. M. (2015). Vegfc regulates bipotential precursor division and Prox1 expression to promote lymphatic identity in zebrafish. *Cell Rep.* **13**, 1828-1841.

Kuchler, A. M., Gjini, E., Peterson-Maduro, J., Cancilla, B., Wolburg, H. and Schulte-Merker, S. (2006). Development of the zebrafish lymphatic system requires VEGFC signaling. *Curr. Biol.* **16**, 1244-1248.

Kwan, K. M., Fujimoto, E., Grabher, C., Mangum, B. D., Hardy, M. E., Campbell, D. S., Parant, J. M., Yost, H. J., Kanki, J. P. and Chien, C.-B. (2007). The Tol2kit: a multisite gateway-based construction kit for Tol2 transposon transgenesis constructs. *Dev. Dyn.* **236**, 3088-3099.

Langenau, D. M., Ferrando, A. A., Traver, D., Kutok, J. L., Hezel, J.-P. D., Kanki, J. P., Zon, L. I., Look, A. T. and Trede, N. S. (2004). In vivo tracking of T cell development, ablation, and engraftment in transgenic zebrafish. *Proc. Natl. Acad. Sci. USA* **101**, 7369-7374.

Lawson, N. D. and Weinstein, B. M. (2002). In vivo imaging of embryonic vascular development using transgenic zebrafish. *Dev. Biol.* **248**, 307-318.

Lee, S. J., Evers, S., Roeder, D., Parlow, A. F., Risteli, J., Risteli, L., Lee, Y. C., Feizi, T., Langen, H. and Nussenzweig, M. C. (2002). Mannose receptor-mediated regulation of serum glycoprotein homeostasis. *Science* **295**, 1898-1901.

Linehan, S. A., Martínez-Pomares, L., Stahl, P. D. and Gordon, S. (1999). Mannose receptor and its putative ligands in normal murine lymphoid and nonlymphoid organs: In situ expression of mannose receptor by selected macrophages, endothelial cells, perivascular microglia, and mesangial cells, but not dendritic cells. *J. Exp. Med.* **189**, 1961-1972.

Martinez-Pomares, L., Hanitsch, L. G., Stillion, R., Keshav, S. and Gordon, S. (2005). Expression of mannose receptor and ligands for its cysteine-rich domain in venous sinuses of human spleen. *Lab. Invest.* **85**, 1238-1249.

Marttila-Ichihara, F., Turja, R., Miiluniemi, M., Karikoski, M., Maksimow, M., Niemela, J., Martinez-Pomares, L., Salmi, M. and Jalkanen, S. (2008). Macrophage mannose receptor on lymphatics controls cell trafficking. *Blood* **112**, 64-72.

Mulligan, T. S. and Weinstein, B. M. (2014). Emerging from the PAC: studying zebrafish lymphatic development. *Microvasc. Res.* **96**, 23-30.

Nicenboim, J., Malkinson, G., Lupo, T., Asaf, L., Sela, Y., Mayseless, O., Gibbs-Bar, L., Senderovich, N., Hashimshony, T., Shin, M. et al. (2015). Lymphatic vessels arise from specialized angioblasts within a venous niche. *Nature* **522**, 56-61.

Okuda, K. S., Astin, J. W., Misa, J. P., Flores, M. V., Crosier, K. E. and Crosier, P. S. (2012). lyve1 expression reveals novel lymphatic vessels and new mechanisms for lymphatic vessel development in zebrafish. *Development* **139**, 2381-2391.

Renshaw, S. A., Loynes, C. A., Trushell, D. M. I., Elworthy, S., Ingham, P. W. and Whyte, M. K. B. (2006). A transgenic zebrafish model of neutrophilic inflammation. *Blood* **108**, 3976-3978.

Rusznyák, I. N., Földi, M. L. and Szabó, G. R. (1967). *Lymphatics and Lymph Circulation; Physiology and Pathology*, 2nd edn. New York: Pergamon Press.

Salmi, M., Karikoski, M., Elima, K., Rantakari, P. and Jalkanen, S. (2013). CD44 binds to macrophage mannose receptor on lymphatic endothelium and supports lymphocyte migration via afferent lymphatics. *Circ. Res.* **112**, 1577-1582.

Swift, M. R., Pham, V. N., Castranova, D., Bell, K., Poole, R. J. and Weinstein, B. M. (2014). SoxF factors and Notch regulate nr2f2 gene expression during venous differentiation in zebrafish. *Dev. Biol.* **390**, 116-125.

Takahashi, K., Donovan, M. J., Rogers, R. A. and Ezekowitz, R. A. B. (1998). Distribution of murine mannose receptor expression from early embryogenesis through to adulthood. *Cell Tissue Res.* **292**, 311-323.

Tammela, T. and Alitalo, K. (2010). Lymphangiogenesis: molecular mechanisms and future promise. *Cell* **140**, 460-476.

Development (2017) 144, 2070-2081 doi:10.1242/dev.145755

Taylor, P. R., Gordon, S. and Martinez-Pomares, L. (2005a). The mannose receptor: linking homeostasis and immunity through sugar recognition. *Trends Immunol.* **26**, 104-110.

Taylor, P. R., Martinez-Pomares, L., Stacey, M., Lin, H.-H., Brown, G. D. and Gordon, S. (2005b). Macrophage receptors and immune recognition. *Annu. Rev. Immunol.* **23**, 901-944.

Torres-Vázquez, J., Gitler, A. D., Fraser, S. D., Berk, J. D., Van, N. P., Fishman, M. C., Childs, S., Epstein, J. A. and Weinstein, B. M. (2004). Semaphorin-plexin signaling guides patterning of the developing vasculature. *Dev. Cell* **7**, 117-123.

Totong, R., Schell, T., Lescroart, F., Ryckebusch, L., Lin, Y.-F., Zygmunt, T., Herwig, L., Krudewig, A., Gershoony, D., Belting, H.-G. et al. (2011). The novel transmembrane protein Tmem2 is essential for coordination of myocardial and endocardial morphogenesis. *Development* **138**, 4199-4205.

Traver, D., Paw, B. H., Poss, K. D., Penberthy, W. T., Lin, S. and Zon, L. I. (2003). Transplantation and in vivo imaging of multilineage engraftment in zebrafish bloodless mutants. *Nat. Immunol.* **4**, 1238-1246.

van Impel, A., Zhao, Z., Hermkens, D. M., Roukens, M. G., Fischer, J. C., Peterson-Maduro, J., Duckers, H., Ober, E. A., Ingham, P. W. and Schulte-Merker, S. (2014). Divergence of zebrafish and mouse lymphatic cell fate specification pathways. *Development* **141**, 1228-1238.

Vanhollebeke, B., Stone, O. A., Bostaille, N., Cho, C., Zhou, Y., Maquet, E., Gauquier, A., Cabochette, P., Fukuhara, S., Mochizuki, N. et al. (2015). Tip cell-specific requirement for an atypical Gpr124- and Reck-dependent Wnt/beta-catenin pathway during brain angiogenesis. *eLife* 4, doi:10.7554/eLife.06489.

Venero Galanternik, M., Stratman, A. N., Jung, H. M., Butler, M. G. and Weinstein, B. M. (2016). Building the drains: the lymphatic vasculature in health and disease. *Wiley Interdiscip. Rev. Dev. Biol.* **5**, 689-710.

Westerfield, M. (2000). *The Zebrafish Book: A Guide for the Laboratory Use of Zebrafish (Danio rerio)*. 4th edn. Eugene: University of Oregon Press.

White, R. M., Sessa, A., Burke, C., Bowman, T., LeBlanc, J., Ceol, C., Bourque, C., Dovey, M., Goessling, W., Burns, C. E. et al. (2008). Transparent adult zebrafish as a tool for in vivo transplantation analysis. *Cell Stem Cell* **2**, 183-189.

Wigle, J. T. and Oliver, G. (1999). Prox1 function is required for the development of the murine lymphatic system. *Cell* **98**, 769-778.

Wong, K. S., Proulx, K., Rost, M. S. and Sumanas, S. (2009). Identification of vasculature-specific genes by microarray analysis of Etsrp/Etv2 overexpressing zebrafish embryos. *Dev. Dyn.* **238**, 1836-1850.

Yaniv, K., Isogai, S., Castranova, D., Dye, L., Hitomi, J. and Weinstein, B. M. (2006). Live imaging of lymphatic development in the zebrafish. *Nat. Med.* **12**, 711-716.

Yaniv, K., Isogai, S., Castranova, D., Dye, L., Hitomi, J. and Weinstein, B. M. (2007). Imaging the developing lymphatic system using the zebrafish. *Novartis Found. Symp.* **283**, 139-148; discussion 148-151, 238-241.

Yoffey, J. M. and Courtice, F. C. (1970). *Lymphatics, Lymph and the Lymphomyeloid Complex*. London, New York: Academic Press.